Gene therapy targeting sustained FGF23-ERK signaling alleviates kidney inflammation

Adrian Salas-Bastos[1#], Claire Bardet[2#], Klaudia Kopper[1,3], Louisa Jauze[4,7], Fanny Collaud[4,7], Amandine Francois[2,4,7], Gaozhi Chen[5,6], Moosa Mohammadi[5,6], Christian Stockmann[1], Lukas Sommer[1], Johannes Loffing[1,3], Giuseppe Ronzitti[4,7]*, Ganesh Pathare[1,3*§]

[1]Institute of Anatomy, University of Zurich, Zurich, Switzerland.
[2]Université de Paris, Institut des maladies musculo-squelettiques, Laboratory Orofacial Pathologies, Imaging and Biotherapies URP2496 and FHU-DDS-Net, Dental School, and Plateforme d'Imagerie du Vivant (PIV), Montrouge, France.
[3]Swiss National Centre of Competence in Research "Kidney Control of Homeostasis", Switzerland; [4]Genethon, 91000 Evry, France.
[5]Oujiang Laboratory (Zhejiang Lab for Regenerative Medicine, Vision, and Brain Health), School of Pharmaceutical Sciences, Wenzhou Medical University, Wenzhou, China.
[6]Institute of Cell Growth Factor, Oujiang Laboratory (Zhejiang Lab for Regenerative Medicine, Vision, and Brain Health), Wenzhou, China.
[7]Université Paris-Saclay, Univ Evry, Inserm, Genethon, Integrare research unit UMR_S951, 91000 Evry, France.

[#] and * contributed equally

[§]**Corresponding author**:
Ganesh Pathare, BVSc, PhD
Institute of Anatomy
University of Zurich
Winterthurerstrasse 190, 8057, CH
Email: ganesh.pathare@anatomy.uzh.ch

Keywords: FGF23, Klotho, Chronic kidney disease (CKD), X-linked hypophosphatemia (XLH), ERK1/2.

Competing Interests

L.J. and G.R. are inventors in a patent concerning the treatment of XLH (WO/2020/212626). All other authors declare no conflict of interest.

ABSTRACT

Fibroblast growth factor 23 (FGF23) levels are highly elevated in patients with chronic kidney disease (CKD); however, whether it serves merely as a biomarker or actively contributes to kidney inflammation remains unclear. Full-length FGF23 is cleaved into C-terminal FGF23 (cFGF23), which acts as a natural antagonist of FGF23 by inhibiting its binding to the FGF receptor (FGFR) and the co-receptor Klotho. Here, we show that chronically elevated FGF23 levels in a mouse model Hyp-Duk cause sustained-ERK signaling and an inflammatory and immune responses in the kidney. cFGF23, delivered via adeno-associated virus (AAV) gene therapy, successfully mitigated sustained-ERK signaling and kidney inflammation in Hyp-Duk mice. On the other hand, acute physiological FGF23 levels *in vitro* elicited transient-ERK signaling with the expression of canonical early-ERK targets (*EGR1, JUNB, FOSB*). Consistent with *in vivo* findings, prolonged pathological FGF23 treatment *in-vitro* revealed sustained-ERK signaling with upregulation of late-ERK targets (*ETV4/5, SPRED1/2, SPRY2/4*) and unique inflammatory and immune gene signatures. These effects were significantly mitigated by FGFR and ERK inhibitors, as well as by recombinant cFGF23 treatment. In summary, chronically high levels of FGF23 induce kidney inflammation through the FGFR-Klotho complex and sustained-ERK activation, which are successfully mitigated by cFGF23 gene therapy.

KEY POINTS

- Fibroblast growth factor 23 (FGF23) levels are highly elevated in patients with chronic kidney disease (CKD). FGF23 is also a potential biomarker for CKD and related cardiovascular disorders, although its role in disease progression remains unclear.
- Our study identifies that chronically elevated FGF23 levels induce sustained-ERK signaling *in-vitro* and *in-vivo*, leading to inflammation and immune signaling pathways in the kidney.
- These untoward effects of FGF23 were significantly suppressed by gene therapy using the C-terminal peptide of FGF23 (cFGF23), a natural FGF23 antagonist, warranting further investigation to confirm its clinical potential in CKD.

INTRODUCTION

The phosphaturic hormone fibroblast growth factor 23 (FGF23) is primarily produced by osteoblasts and osteocytes[1–3]. FGF23 mediates its phosphaturic effects by inducing asymmetric dimerization of its cognate FGF receptors (FGFR) in the kidneys in a Klotho and heparan sulfate (HS) dual coreceptor fashion[2,4–6]. The 1:2:1:1 FGF23-FGFR-Klotho-HS signaling complex rapidly triggers ERK signaling thus inducing expression of immediate early genes such as *Egr1, Fos* and *Jun,* necessary for regulating mineral metabolism[6–8]. Klotho is a single pass transmembrane protein and is primarily expressed in the kidneys as mice with a kidney-specific Klotho ablation have a similar phenotype as global Klotho knockout mice[9]. Klotho is also expressed in in the brain, parathyroid glands, and gonads, albeit in lower levels compared to the kidney[10]. Extracellular shedding results in soluble form of Klotho (sKlotho) that is found in blood, urine, and cerebrospinal fluid[11]. sKlotho in supraphysiologic levels can mimic some of the effects of transmembrane Klotho[6,12]. FGF23's bioactivity is principally regulated by a proteolytic cleavage, resulting in inactive larger N-terminal (nFGF23) and C-terminal fragments (cFGF23). Intact (iFGF23 or simply FGF23), nFGF23 and cFGF23 coexist in the circulation[13,14].The isolated cFGF23 peptide inhibits FGF23-Klotho binding thereby suppressing FGF23-mediated regulation of mineral metabolism[15,16].

FGF23 levels are massively elevated in chronic kidney disease (CKD) patients and have been associated with inflammation, cardiovascular disease, morbidity and mortality[17–21]. The fact that chronic administration of cFGF23 alleviated renal and cardiovascular pathobiology in a rodent model of CKD lends credence to the notion that the association between high FGF23 and adverse events is more than a mere association but in fact signifies causality[22]. Whether elevated FGF23 causes kidney inflammation in CKD is not clear[23]. Inflammatory cytokines such as IL-6 and TNF-α are often elevated in CKD patients and may upregulate FGF23 expression in bone, as well as in immune cells and tissues that do not normally express FGF23[17,24–26]. Conversely, elevated FGF23 has been shown to induce inflammation in hepatocytes and immune cells, which do not express Klotho[25,27–29]. The Klotho-independent actions of FGF23 contradict the functional and structural data that proposes the essential role of Klotho in FGF23 function[5,6,12].

FGF23 is elevated in numerous human genetic diseases of hypophosphatemia, including X-linked hypophosphatemia (XLH), which is caused by inactivating mutations in the *PHEX* gene[30,31]. The clinical symptoms of XLH are growth retardation, leg bowing, rickets, osteomalacia, bone pain, and dental illness. Many of these symptoms are phenocopied in various murine models of XLH, whether arising from a spontaneous mutation such as the *Hyp-Duk* mouse or generated by inactivating the *Phex* gene[16,30,32]. To date, no inflammatory lesions have been reported in the kidneys or heart of XLH patients and mouse models who have lifelong elevated FGF23 levels[32–35]. However, recently, one study found that XLH patients have elevated circulatory inflammatory markers, suggesting a possible link between chronic FGF23 elevation and inflammation in XLH[36].

Physiological regulators like dietary phosphate, vitamin-D and other hormones stimulate FGF23 transiently within a narrow physiologic range[37]. In contrast, CKD and XLH patients have chronically highly elevated FGF23 levels[17,18,20,21,37]. The differential effects of low-transitory (~physiological) versus

high-prolonged (~pathological) FGF23 levels on temporal phases of ERK activation are unclear. Continued FGF23 availability for FGFR-Klotho binding in the kidney may lead to sustained-ERK activity, but this has not been demonstrated yet. Sustained-ERK activation regulates several transcription factors and gene signatures that govern inflammation and immune responses[38,39]. We hypothesize that chronically elevated FGF23 levels may cause inflammation and immune gene signatures via sustained-ERK signaling, expanding from the canonical role of FGF23 as a regulator of mineral metabolism.

RESULTS

1. Chronically elevated FGF23 levels in mice induce sustained-ERK signaling, inflammation and immune gene signatures in the kidneys, which are mitigated by cFGF23 gene therapy.

An adeno-associated virus (AAV) vector was generated to secrete human cFGF23 from the liver and increase circulating cFGF23 (AAV-cFGF23)[16]. Fig. 1A illustrates the experimental approach used in this study. As expected, serum FGF23 levels in Hyp-Duk mice were significantly higher than in WT mice (Fig. 1B). Circulating human cFGF23 levels were significantly increased in AAV-cFGF23-treated Hyp-Duk mice (Fig. 1C), while this assay did not detect endogenous mouse cFGF23 due to species specificity (Fig. S1). RNA-seq was performed on kidney samples of WT, Hyp-Duk and Hyp-Duk mice treated with AAV-cFGF23 (cFGF23-Hyp-Duk).

The number of DEGs (p-value<0.05) in the kidneys of Hyp-Duk and cFGF23-Hyp-Duk are shown in Fig. S2 (datasets S1/2). Volcano plots illustrate DEGs between the kidneys of Hyp-Duk versus WT and AAV-cFGF23-Hyp-Duk versus Hyp-Duk mice (Fig. 1D). Notably, many canonical FGF23 targets, such as *Dnase1*, *Slc34a1*, *Kl*, and *Ace2*, were downregulated in the kidney of Hyp-Duk mice but upregulated in the kidneys of cFGF23-Hyp-Duk mice, validating the gene therapy approach (Fig. 1D). Previously unrecognized ERK and inflammatory targets, such as *Etv4*, *Stat3*, *Ets1*, and *Nfkb2*, were significantly upregulated in the kidneys of Hyp-Duk mice but downregulated the kidneys of cFGF23-Hyp-Duk mice (Fig. 1D). Notably, only late-ERK targets were significantly upregulated in the kidneys of Hyp-Duk mice and completely or partially rescued in the kidneys of cFGF23-Hyp-Duk mice (Fig. 1E/S3). Early-ERK targets remained unchanged in the kidneys of Hyp-Duk mice (Fig. 1F).

To determine if sustained-ERK activation also regulates inflammatory and immune gene signatures as observed *in vitro*, we intersected DEGs in the kidneys of Hyp-Duk mice with the immunological database ImmPort. The results showed that 20.5% of the total number of DEGs corresponded to ImmPort annotated genes (Fig. 1G). Notably, cFGF23 gene therapy rescued 27.4% of the affected DEGs (Fig. 1H). The rescued genes are highlighted in the heatmap (Fig. 1I). GO enrichment analysis identified 277 pathways that were significantly (padj<0.05) upregulated in the kidneys of Hyp-Duk mice and rescued in the kidneys of cFGF23-Hyp-Duk mice (datasets S3/4/5). Many of these pathways were associated with inflammation and immune responses. For instance, the ERK-mediated *Ras pathway, inflammatory and immune responses, Wnt signaling* and *complement activation* were significantly upregulated in the kidneys of Hyp-Duk mice and rescued in the kidneys of cFGF23-Hyp-Duk mice (Fig. 1J; datasets S3/4/5). The inflammatory *JAK-STAT cascade* and *TNF cytokine production* were significantly upregulated in the kidney of Hyp-Duk mice and partially rescued in the kidney of cFGF23-Hyp-Duk mice

(Fig. 1J; datasets S3/4/5). This list is not exhaustive; for the full list of genes, refer to the GO pathways datasets S3/4/5.

Fig. 1K/L show selected genes implicated in inflammatory and immune gene signatures that were upregulated in the kidneys of Hyp-Duk mice and reversed in the kidneys of cFGF23-Hyp-Duk mice. Genes involved in paracrine FGF signaling, such as *Fgf10*, *Hspg2*, and *Fgf2*, were significantly upregulated in the kidneys of Hyp-Duk mice and rescued in the kidneys of cFGF23-Hyp-Duk mice (Fig. S4). We found canonical mineral metabolism targets of FGF23 in the kidneys of Hyp-Duk mice, such as *Cyp27b1*, *Cyp24a1*, *Slc34a1*, and *Kl*, as well as several previously unrecognized gene targets, including *Slc34a2*, *Pth1r*, and *Calb1* (Fig. S5). Fig. S6 summarizes the pathways upregulated in the renal transcriptional signature associated with skeletal defects in Hyp-Duk mice. *Lcn2* upregulation in Hyp-Duk kidneys prompted us to measure urinary neutrophil gelatinase-associated lipocalin (NGAL), a marker of kidney inflammation and injury. Urinary NGAL levels were significantly elevated in Hyp-Duk mice and were rescued following AAV-cFGF23 treatment (Fig. 1M).

2. Sustained-ERK activation *in-vitro* occurs with high, but not low, FGF23 concentrations.

HEK293 (HEK^{Wt}) cells endogenously express FGFR1-4 but not Klotho. We stably transfected these cells with Klotho to generate a stable Klotho HEK293 cell line (HEK^{Kl}). HEK^{Wt} and HEK^{Kl} cells are excellent models for studying Klotho-independent and Klotho-dependent FGF23 functions, respectively[12,40]. The activation of pERK1/2 by FGF23 in the presence of Klotho was confirmed (Fig. S8). Treatment with 0.5 nM FGF23, which resembles the physiological condition, in HEK^{Kl} cells, resulted in a transient increase in pERK1/2 that was visible after 15 minutes but not at 24 hours (Fig. 2A, left panel). Treatment with 10 nM FGF23, a higher concentration mimicking the pathological levels, led to pERK1/2 activation at 15 minutes which persists to 24 hours (Fig. 2A, right panel). FGF23 concentrations exceeding 5 nM resulted in sustained pERK1/2 activation (Fig. 2B). To determine the precise time points for the transcriptomics analysis, we used both low and high FGF23 concentrations and measured *EGR1* mRNA as a canonical marker for FGF23 signaling. Upon 0.5 nM FGF23 treatment in HEK^{Kl} cells, *EGR1* mRNA peaked at 1 hour, with no statistically significant difference at 24 hours compared to the control HEK^{Wt}-treated cells (Fig. 2C). Notably, 10 nM FGF23 treatment followed almost a similar trend except a 13-fold higher *EGR1* levels were still observed after 24 hours (Fig. 2D/E). Both pERK1/2 and *EGR1* levels remained unchanged in HEK^{Wt} cells throughout the treatment periods indicating the absolute requirement of the co-receptor Klotho for FGF23 signaling.

3. Pathologically elevated FGF23 levels induce sustained-ERK signaling and inflammation-related gene signatures *in vitro*.

To evaluate the transcriptomic profile after treatment with physiological or pathological FGF23 concentrations, we performed RNA-seq analysis as illustrated in Fig. 3A. Physiological FGF23 treatment in HEK^{Wt} cells did not affect the transcriptome (Fig. 3B, left panel; dataset S6; and Fig. S9A). Physiological FGF23 treatment in HEK^{Kl} cells led to 64 differentially expressed genes (DEGs), with 61 upregulated and 3 downregulated (Fig. 3B, right panel; dataset S7). Canonical early genes such as *EGR1, FOS* and *JUNB* were among the top upregulated genes, validating our approach. Although

pathological FGF23 concentrations in HEK^{Wt} cells resulted in few DEGs, these showed log2FC<1, suggesting a minimal non-Klotho-dependent effect of FGF23 (Fig. 3C, left panel; dataset S8). While pathological FGF23 treatment in HEK^{Kl} cells demonstrated a robust transcriptomics response (Fig. 3C, right panel; dataset S9).

The physiological and pathological FGF23 treatments in HEK^{Kl} cells upregulated several ERK target genes (Fig. S10). Early immediate genes like *EGR1, FOS, FOSB, JUNB* and *JUND* were significantly upregulated by physiological FGF23 compared to pathological FGF23 treatment *(early-ERK targets;* Fig. 3D and S11). *EGR1* expression was 150-fold higher after physiological FGF23 treatment, but only 10-fold higher in pathological conditions, indicating its primary role in transient-ERK activity. In contrast, *JUNB* and *FOSB* were unchanged by pathological FGF23 treatment, suggesting they are strictly *early-ERK targets* (Fig. S10). Conversely, ERK targets such as *DUSP4/6*, *ETV1/4/5*, *SPRED1/2*, and *SPRY2/4* were either unchanged or significantly upregulated by pathological FGF23 compared to physiological FGF23 treatment (Fig. 3E, S11). These transcripts were identified as *late-ERK targets*. Among these, *ETV1/4/5* and *SPRED1/2* were unchanged by physiological FGF23, indicating they are strictly *late-ERK targets* (Fig. S11).

As depicted in the Venn diagram, 88 and 40 DEGs were exclusively regulated by pathological and physiological FGF23, respectively, with 24 DEGs overlapping (Fig. 3F). This suggests that physiological and pathological FGF23 levels drive divergent transcriptomic responses. Analysis of the Gene ontology (GO) pathways of biological processes linked to genes upregulated by pathological FGF23 identified several processes implicated in inflammation and immune response (Fig. 3G, red arrows. A complete list of GO pathways is available in dataset S11). Therefore, we intersected DEGs regulated by pathological FGF23 with the immunological database ImmPort (https://www.immport.org). This analysis retrieved a set of genes linked to inflammatory and immune signatures, which are highlighted in the heatmap (Fig. 3H). Block 1 of the heatmap shows the inflammatory and immune gene signatures exclusively regulated by pathological FGF23, while block 2 shows genes regulated by both pathological and physiological FGF23. Representative inflammatory and immune gene signatures (*TNFRSF9/12A*, *GDF15*, *ANXA1*, and *TGFB1*) by pathological FGF23 (block 1) are highlighted in Fig. 3I. Notably, the early- and late-ERK targets, as well as novel FGF23 targets implicated in inflammatory and immune gene signatures, are upregulated only in HEK^{Kl} cells and not in HEK^{Wt} cells (Fig. 3I; Fig. S10/S11). Several transcripts implicated in sustained-ERK signaling and inflammatory and immune gene signatures were identical in HEK^{Kl} cells and the kidneys of Hyp-Duk mice (Fig. S12/S13).

4. FGF23-mediated inflammatory and immune gene signatures are mediated by FGFR and ERK *in vitro.*

We used blockers of FGFR (PD173074) and MEK (U0126) to investigate the roles of FGFR and ERK in the effects mediated by pathological FGF23. The mRNA levels of newly identified targets were quantified using qRT-PCR. Pretreatment with either FGFR or MEK inhibitors completely reversed the FGF23-mediated upregulation of the early-ERK target *EGR1* (Fig. 4A, left panel). The late-ERK target *ETV4* was also entirely blocked by the FGFR inhibitor, while it was partially but significantly blocked by

the MEK inhibitor (Fig. 4A, right panel). Next, we quantified the inflammation and immune targets such as *TNFRSF9/12A, GDF15, ANXA1,* and *TGFB1*. FGF23-mediated upregulation of mRNA levels of these genes were completely abrogated by FGFR inhibitors and partially but significantly reversed by MEK inhibitors (Fig. 4B). This implies that there is divergence of signaling post FGFR to different pathways.

5. cFGF23 mitigates FGF23-mediated inflammatory and immune gene signatures *in vitro*.

The presence of Klotho on the surface was crucial for the transcriptomic response to both physiological and pathological FGF23 levels. To investigate whether FGF23 binding to Klotho was specifically involved in this response, we used recombinant human cFGF23 peptide to prevent FGF23 binding to the FGFR-Klotho co-receptor complex[15] (Fig. 5A). Pretreatment with cFGF23 blocked the FGF23-mediated upregulation of the early-ERK target *EGR1* as well as the late-ERK target *ETV4* in a dose-dependent manner (Fig. 5B). A high dose of cFGF23 (10 μM) alone did not affect *EGR1* mRNA levels; however, it slightly but significantly increased *ETV4* mRNA levels (Fig. 5B, right panel). Next, we validated the inflammation and immune targets such as *TNFRSF9/12A*, *GDF15*, *ANXA1*, and *TGFB1* using qPCR. Similar to ERK targets, FGF23 upregulated these genes, which were partially rescued by cFGF23 co-treatment in a dose-dependent manner (Fig. 5C). Interestingly, cFGF23 alone did not affect the mRNA expressions of any of the inflammatory and immune targets, suggesting that potential "off-target" effects of cFGF23 are probably limited to *ETV4* mRNA (Fig. 5C).

DISCUSSION:

Our study provides three salient findings: (i) chronically elevated FGF23 levels in mice induce sustained-ERK activation and inflammation in the kidney; (ii) cFGF23 gene therapy mitigates sustained-ERK signaling and associated inflammatory responses by blocking FGFR-Klotho binding; and (iii) FGF23 levels drive temporal ERK signaling dynamics *in-vitro*, with acute physiological levels triggering transient-ERK activation and chronic pathological levels inducing sustained-ERK activation and inflammatory gene signatures.

We found that the early-ERK targets were unchanged in the kidneys of Hyp-Duk mice, while the Hyp-Duk kidneys exhibited elevated late-ERK targets (sustained-ERK signaling) along with activation of inflammatory and immune signaling pathways. The structurally related isoforms, ERK1 and ERK2, were the first MAPKs identified, based on early observations of their rapid and reversible phosphorylation in response to growth factor stimulation[41]. Activated ERK translocates into the nucleus and stimulates transcription factors associated with immediate early genes (*Egr*, *Fos*, and *Jun* families)[42–44]. This type of transient-ERK activation is known to participate in FGF23-mediated mineral homeostasis in the kidney[7,8,45,46]. Conversely, chronically high FGF23 levels in Hyp-Duk mice elevated late-ERK targets (*Etv*, *Spred*, *Spry* families) likely due to continuous and irreversible translocation of ERK into the nucleus. The sustained-ERK signaling is known to trigger inflammatory and immune responses by activating transcription factors like Nuclear Factor kappa-light-chain-enhancer of activated B cells (NF-κB), ETS-like gene 1 (Elk1), cAMP response element-binding protein (CREB), Signal transducers and activators of transcription (STAT)[38,39,47]. Indeed, many proinflammatory pathways, such as *Ras*, *JAK*-

STAT cascade, *Wnt signaling*, *TNF regulation, leukocyte activation*, and *cytokine production*, were significantly upregulated in the kidneys of Hyp-Duk mice and were fully or partially rescued by cFGF23 gene therapy. Consistently, genes associated with inflammatory and immune cell infiltration, including *Adgre1* (F4/80), *Ptprc* (CD45), and *H2-Aa* (MHC-II), were significantly upregulated in the kidneys of Hyp-Duk mice and may contribute to the proinflammatory responses.

Renal NGAL expression and its urinary levels, a marker of kidney injury and inflammation, were significantly elevated in Hyp-Duk mice and were rescued by cFGF23 gene therapy. Classical fibrosis markers, such as *Col1a1* and *Col3a1*, were upregulated in the kidneys of Hyp-Duk mice, whereas the conventional kidney injury marker *Havcr1* (KIM-1) was not elevated (datasets S1), suggesting subclinical kidney injury. Consistently, as reported in prior studies, plasma BUN and creatinine levels were unchanged in Hyp mice[48,49]. This implies that elevated FGF23 alone is probably inadequate to cause renal insufficiency without a second hit, such as aging, hypertension, hyperphosphatemia, uremia, or other CKD-related factors. While this manuscript was in preparation, Bockmann and colleagues reported significant renal comorbidities in pediatric XLH patients, including reduced eGFR and elevated urinary markers of glomerular and tubular injury and inflammation[50]. Both XLH patients and mouse models with elevated FGF23 may exhibit subclinical or undetected kidney injury driven by sustained-ERK signaling and associated inflammation.

Our *in vitro* data confirmed that prolonged FGF23 binding to FGFR-Klotho causes sustained-ERK activation and upregulation late-ERK transcripts. MEK inhibitor rescued FGF23-mediated sustained-ERK signaling as well as inflammatory and immune gene signatures. Notably, the newly identified proinflammatory FGF23 signaling targets in HEK^{KI} cells (*TGFB1, TNFRSF9/12A8, ANXA19,* and *GDF1510*) are also elevated in human CKD patients[51–54]. The ERK and inflammatory and gene signatures in the kidneys of Hyp-Duk mice showed significant overlap with those in HEK^{KI} cells but were not completely identical (Fig S12/13), likely due to species specificity and differences between cell-autonomous and systemic inflammatory effects.

FGFR inhibitor completely abolished ERK signaling and inflammatory and immune gene signatures. Both Klotho and FGFRs are expressed in renal proximal and distal tubules, participating in the canonical effects of FGF23 in mineral metabolism[10,55,56]. FGFR1/3/4 are implicated in FGF23-Klotho signaling[6,12]. Notably, only FGFR4 was significantly downregulated, while FGFR1/3 remained unchanged in the kidneys of Hyp-Duk mice (Fig. S7). The specific FGFRs mediating the inflammatory FGF23-ERK signaling is presently unclear. Previous studies have shown that both FGFR and ERK inhibition in Hyp mice corrected mineral metabolism and skeletal phenotype[46,57]. It is tempting to speculate that these inhibitors might also block the inflammatory gene signatures triggered by FGF23-mediated sustained-ERK signaling in the kidneys.

A hallmark of our study is that cFGF23 mitigates FGF23-mediated sustained-ERK signaling, and inflammatory gene signatures both *in vitro* and *in vivo*. In Hyp-Duk mice, AAV-cFGF23 treatment led to high levels of human cFGF23 in mouse serum, effectively correcting inflammatory and immune gene signatures. The structure of the FGF23-FGFR-Klotho complex shows that the C-terminal region of

FGF23 binds into an extended groove between the Kl1 and Kl2 domains of Klotho[6,12]. The isolated cFGF23 peptide can bind specifically into this groove, competitively inhibiting Klotho-dependent FGF23 signaling[15]. Thus, cFGF23 likely mitigated Klotho-dependent FGF23 actions in Hyp-Duk mice. Supporting our findings, a previous study showed no change in inflammation-related gene expression in the heart and liver of Hyp mice, where Klotho is not expressed[32]. These findings corroborate our *in vitro* data, concluding Klotho is needed for FGF23 signaling. There was no transcriptomic response to physiological FGF23 levels in HEK^{Wt} cells. Few genes showed subtle changes upon pathological FGF23 levels in HEK^{Wt} cells. However, ERK activation and inflammatory and immune gene signatures were observed only in HEK^{Kl} cells. These findings largely align with recent studies demonstrating that Klotho is essential for FGF23 signaling[6,12]. On the other hand, elevated FGF23 levels were previously shown to trigger inflammation in extrarenal cells such as immune cells and hepatocytes, independent of Klotho[25,27–29]. At present our findings cannot refute Klotho-independent FGF23 actions in inflammation[19,40].

Paracrine FGFs like FGF2/10 directly activate ERK via FGFR and heparan sulfate (*Hspg2*) independent of Klotho[58]. We found that *Fgf2*, *Fgf10* and *Hspg2* were significantly upregulated in the kidneys of Hyp-Duk mice and rescued by cFGF23 treatment. Enhanced paracrine FGF signaling in the kidneys is likely due to chronically elevated FGF23 levels, consistent with previous reports showing upregulated FGF2 levels in the bones of Hyp mice[59]. Persistent paracrine FGF signaling could also be proinflammatory[58], and there might be cross-talk with endocrine FGF23 signaling during chronic FGF23 elevation.

The FGF23-mediated proinflammatory sustained-ERK signaling proposed here may have significant implications in human CKD. Preclinical studies suggest that MEK Inhibitor ameliorates CKD by suppressing ERK signaling[60–62]. It remains to be investigated whether the effect was specifically due to blocking FGF23-mediated sustained-ERK signaling. Our study suggests that the beneficial effects of MEK inhibitor in CKD, at least partly, are mediated by blocking FGF23-mediated sustained-ERK pathway. Importantly, recent studies demonstrated that cFGF23 treatment could improve anemia, heart function and some kidney functions in murine models of CKD[22,63,64]. Gene therapy with AAV-cFGF23 may provide a better efficacy due to its known capacity to release steady levels of cFGF23 in circulation without the peak-and-trough effect known to be associated with protein therapy[16].

In conclusion, pathologically elevated FGF23 levels trigger inflammatory and immune gene signatures through the FGFR-Klotho complex and sustained-ERK activation. These untoward effects of FGF23 were significantly mitigated by cFGF23 gene therapy, warranting further investigation to confirm its clinical potential.

Statistics

All the values are expressed as arithmetic means ± SEM, where n represents number of independent experiments (biological replicates). An unpaired Student's t test was used for comparisons between the groups using GraphPad Prism. In cases where the p value is not mentioned, the following applies: ns (not significant) $p > 0.05$, $*p \leq 0.05$, $**p < 0.01$, and $***p < 0.001$.

Illustrations

Graphical illustrations were created using a licensed version of Biorender software.

DATA AVAILABILITY

All the relevant data associated with the current study can be found in the main text or supplementary datasets. The raw RNA-seq data used in this publication have been deposited in NCBI Gene Expression Omnibus and are accessible through GEO series accession numbers GSE248734 and GSE269823. All data are available from the authors upon reasonable request.

ACKNOWLEDGMENTS

This work was supported by the Swiss National Science Foundation through the National Center of Competence in Research NCCR Kidney.CH [grant number N-403-03-55 (to G. P.)], Clinical Research Priority Program HYpertension REsearch NEtwork (CRPP HYRENE) of the University of Zurich (to J. L.), National Natural Science Foundation of China (82073705 & 82273842 to G.C.), Natural Science Foundation for International Senior Scientists (32350710196 to M.M.), Oujiang laboratory startup fund (OJQD2022007 to M.M.), Kungpeng Action Plan award (to M.M.), Natural Science Funding of Zhejiang Province (LR22H300002 to G.C.). The authors thank Prof. Orson Moe and Johanne Pastor from the University of Texas Southwestern Medical Center, Dallas, Texas, USA, for their critical feedback on the manuscript. Part of this manuscript was uploaded as a preprint on bioRxiv on January 20, 2024 (https://doi.org/10.1101/2024.01.18.576116).

AUTHORS CONTRIBUTIONS

GP conceptualized the study; ASB, CB, GR and GP designed the study; ASB, CB, KK, LJ, FC, AF and GP performed the study; GC, MM and JL contributed new reagents/analytic tools; ASB, CB, KK, LJ, FC, AF GC, MM, CS, LS, JL, GR and GP analyzed the data; GP wrote the manuscript; ASB, CB, KK, LJ, FC, AF GC, MM, CS, LS, JL and GR reviewed and edited the manuscript; GP and JL were responsible for funding acquisition; GP was responsible for supervision.

440 **REFERENCES**

441 1. Feng, J. Q., Ward, L. M., Liu, S., Lu, Y., Xie, Y., Yuan, B., Yu, X., Rauch, F., Davis, S. I., Zhang, S., Rios,
442 H., Drezner, M. K., Quarles, L. D., Bonewald, L. F. & White, K. E. Loss of DMP1 causes rickets and
443 osteomalacia and identifies a role for osteocytes in mineral metabolism. *Nat. Genet.* **38**, 1310–1315
444 (2006).

445 2. Shimada, T., Mizutani, S., Muto, T., Yoneya, T., Hino, R., Takeda, S., Takeuchi, Y., Fujita, T., Fukumoto,
446 S. & Yamashita, T. Cloning and characterization of FGF23 as a causative factor of tumor-induced
447 osteomalacia. *Proc. Natl. Acad. Sci. U. S. A.* **98**, 6500–6505 (2001).

448 3. Radvanyi, Z., Yoo, E. J., Kandasamy, P., Salas-Bastos, A., Monnerat, S., Refardt, J., Christ-Crain, M.,
449 Hayashi, H., Kondo, Y., Jantsch, J., Rubio-Aliaga, I., Sommer, L., Wagner, C. A., Hediger, M. A., Kwon,
450 H. M., Loffing, J. & Pathare, G. Extracellular sodium regulates fibroblast growth factor 23 (FGF23)
451 formation. *J. Biol. Chem.* 105480 (2023) doi:10.1016/J.JBC.2023.105480.

452 4. Shimada, T., Hasegawa, H., Yamazaki, Y., Muto, T., Hino, R., Takeuchi, Y., Fujita, T., Nakahara, K.,
453 Fukumoto, S. & Yamashita, T. FGF-23 is a potent regulator of vitamin D metabolism and phosphate
454 homeostasis. *J. Bone Miner. Res.* **19**, 429–435 (2004).

455 5. Urakawa, I., Yamazaki, Y., Shimada, T., Iijima, K., Hasegawa, H., Okawa, K., Fujita, T., Fukumoto, S. &
456 Yamashita, T. Klotho converts canonical FGF receptor into a specific receptor for FGF23. *Nature* **444**,
457 770–774 (2006).

458 6. Chen, L., Fu, L., Sun, J., Huang, Z., Fang, M., Zinkle, A., Liu, X., Lu, J., Pan, Z., Wang, Y., Liang, G., Li,
459 X., Chen, G. & Mohammadi, M. Structural basis for FGF hormone signalling. *Nature* **618**, 862–870
460 (2023).

461 7. Portale, A. A., Zhang, M. Y. H., David, V., Martin, A., Jiao, Y., Gu, W. & Perwad, F. Characterization of
462 FGF23-Dependent Egr-1 Cistrome in the Mouse Renal Proximal Tubule. *PLoS One* **10**, e0142924
463 (2015).

464 8. Ni, P., Clinkenbeard, E. L., Noonan, M. L., Richardville, J. M., McClintick, J., Hato, T., Janosevic, D.,
465 Cheng, Y. H., El-Achkar, T. M., Eadon, M. T., Dagher, P. C. & White, K. E. Targeting fibroblast growth
466 factor 23-responsive pathways uncovers controlling genes in kidney mineral metabolism. *Kidney Int.* **99**,
467 598–608 (2021).

468 9. Lindberg, K., Amin, R., Moe, O. W., Hu, M.-C., Erben, R. G., Östman Wernerson, A., Lanske, B.,
469 Olauson, H. & Larsson, T. E. The Kidney Is the Principal Organ Mediating Klotho Effects. *J. Am. Soc.*
470 *Nephrol.* **25**, 2169–2175 (2014).

471 10. Kuro-o, M., Matsumura, Y., Aizawa, H., Kawaguchi, H., Suga, T., Utsugi, T., Ohyama, Y., Kurabayashi,
472 M., Kaname, T., Kume, E., Iwasaki, H., Iida, A., Shiraki-Iida, T., Nishikawa, S., Nagai, R. & Nabeshima,
473 Y. I. Mutation of the mouse klotho gene leads to a syndrome resembling ageing. *Nature* **390**, 45–51
474 (1997).

475 11. Kurosu, H., Yamamoto, M., Clark, J. D., Pastor, J. V., Nandi, A., Gurnani, P., McGuinness, O. P.,
476 Chikuda, H., Yamaguchi, M., Kawaguchi, H., Shimomura, I., Takayama, Y., Herz, J., Kahn, C. R.,
477 Rosenblatt, K. P. & Kuro-O, M. Suppression of aging in mice by the hormone Klotho. *Science (80-.).*
478 **309**, 1829–33 (2005).

479 12. Chen, G., Liu, Y., Goetz, R., Fu, L., Jayaraman, S., Hu, M. C., Moe, O. W., Liang, G., Li, X. &
480 Mohammadi, M. α-Klotho is a non-enzymatic molecular scaffold for FGF23 hormone signalling. *Nature*
481 **553**, 461–466 (2018).

482 13. White, K. E., Evans, W. E., O'Riordan, J. L. H., Speer, M. C., Econs, M. J., Lorenz-Depiereux, B.,
483 Grabowski, M., Meitinger, T. & Strom, T. M. Autosomal dominant hypophosphataemic rickets is
484 associated with mutations in FGF23. *Nat. Genet.* **26**, 345–348 (2000).

485 14. Larsson, T., Davis, S. I., Garringer, H. J., Mooney, S. D., Draman, M. S., Cullen, M. J. & White, K. E.
486 FGF23 mutants causing familial tumoral calcinosis are differentially processed. *Endocrinology* **146**,
487 3883–3891 (2005).

488 15. Goetz, R., Nakada, Y., Hu, M. C., Kurosu, H., Wang, L., Nakatani, T., Shi, M., Eliseenkova, A. V.,
489 Razzaque, M. S., Moe, O. W., Kuro-o, M. & Mohammadi, M. Isolated C-terminal tail of FGF23 alleviates
490 hypophosphatemia by inhibiting FGF23-FGFR-Klotho complex formation. *Proc Natl Acad Sci U S A* **107**,
491 407–412 (2010).

492 16. Zhukouskaya, V. V., Jauze, L., Charles, S., Leborgne, C., Hilliquin, S., Sadoine, J., Slimani, L., Baroukh,
493 B., van Wittenberghe, L., Danièle, N., Rajas, F., Linglart, A., Mingozzi, F., Chaussain, C., Bardet, C. &
494 Ronzitti, G. A novel therapeutic strategy for skeletal disorders: Proof of concept of gene therapy for X-
495 linked hypophosphatemia. *Sci. Adv.* **7**, (2021).

496 17. Mendoza, J. M., Isakova, T., Ricardo, A. C., Xie, H., Navaneethan, S. D., Anderson, A. H., Bazzano, L.
497 A., Xie, D., Kretzler, M., Nessel, L., Lee Hamm, L., Negrea, L., Leonard, M. B., Raj, D. & Wolf, M.
498 Fibroblast growth factor 23 and Inflammation in CKD. *Clin. J. Am. Soc. Nephrol.* **7**, 1155–1162 (2012).

499 18. Wallquist, C., Mansouri, L., Norrbäck, M., Hylander, B., Jacobson, S. H., Larsson, T. E. & Lundahl, J.
500 Associations of Fibroblast Growth Factor 23 with Markers of Inflammation and Leukocyte Transmigration
501 in Chronic Kidney Disease. *Nephron* **138**, 287–295 (2018).

502 19. Faul, C., Amaral, A. P., Oskouei, B., Hu, M. C., Sloan, A., Isakova, T., Gutiérrez, O. M., Aguillon-Prada,
503 R., Lincoln, J., Hare, J. M., Mundel, P., Morales, A., Scialla, J., Fischer, M., Soliman, E. Z., Chen, J., Go,
504 A. S., Rosas, S. E., Nessel, L., *et al.* FGF23 induces left ventricular hypertrophy. *J. Clin. Invest.* **121**,
505 4393–4408 (2011).

506 20. Gutiérrez, O. M., Mannstadt, M., Isakova, T., Rauh-Hain, J. A., Tamez, H., Shah, A., Smith, K., Lee, H.,
507 Thadhani, R., Jüppner, H. & Wolf, M. Fibroblast growth factor 23 and mortality among patients
508 undergoing hemodialysis. *N. Engl. J. Med.* **359**, 584–592 (2008).

509 21. Isakova, T., Xie, H., Yang, W., Xie, D., Anderson, A. H., Scialla, J., Wahl, P., Gutiérrez, O. M.,
510 Steigerwalt, S., He, J., Schwartz, S., Lo, J., Ojo, A., Sondheimer, J., Hsu, C. Y., Lash, J., Leonard, M.,
511 Kusek, J. W., Feldman, H. I., *et al.* Fibroblast growth factor 23 and risks of mortality and end-stage renal
512 disease in patients with chronic kidney disease. *JAMA* **305**, 2432–2439 (2011).

513 22. Hu, M. C., Reneau, J. A., Shi, M., Takahashi, M., Chen, G., Mohammadi, M. & Moe, O. W. C-terminal
514 fragment of fibroblast growth factor 23 improves heart function in murine models of high intact fibroblast
515 growth factor 23. *Am. J. Physiol. Renal Physiol.* **326**, F584–F599 (2024).

516 23. Fitzpatrick, E. A., Han, X., Xiao, Z. & Quarles, L. D. Role of fibroblast growth factor-23 in innate immune
517 responses. *Front. Endocrinol. (Lausanne).* **9**, 372263 (2018).

518 24. Egli-Spichtig, D., Imenez Silva, P. H., Glaudemans, B., Gehring, N., Bettoni, C., Zhang, M. Y. H., Pastor-
519 Arroyo, E. M., Schönenberger, D., Rajski, M., Hoogewijs, D., Knauf, F., Misselwitz, B., Frey-Wagner, I.,
520 Rogler, G., Ackermann, D., Ponte, B., Pruijm, M., Leichtle, A., Fiedler, G.-M., *et al.* Tumor necrosis factor
521 stimulates fibroblast growth factor 23 levels in chronic kidney disease and non-renal inflammation. *Kidney*
522 *Int.* **96**, 890–905 (2019).

523 25. Masuda, Y., Ohta, H., Morita, Y., Nakayama, Y., Miyake, A., Itoh, N. & Konishi, M. Expression of Fgf23 in
524 Activated Dendritic Cells and Macrophages in Response to Immunological Stimuli in Mice. *Biol. Pharm.*
525 *Bull.* **38**, 687–693 (2015).

526 26. Ito, N., Wijenayaka, A. R., Prideaux, M., Kogawa, M., Ormsby, R. T., Evdokiou, A., Bonewald, L. F.,
527 Findlay, D. M. & Atkins, G. J. Regulation of FGF23 expression in IDG-SW3 osteocytes and human bone
528 by pro-inflammatory stimuli. *Mol. Cell. Endocrinol.* **399**, 208–218 (2015).

529 27. Singh, S., Grabner, A., Yanucil, C., Schramm, K., Czaya, B., Krick, S., Czaja, M. J., Bartz, R., Abraham,
530 R., Di Marco, G. S., Brand, M., Wolf, M. & Faul, C. Fibroblast growth factor 23 directly targets
531 hepatocytes to promote inflammation in chronic kidney disease. *Kidney Int.* **90**, 985–996 (2016).

532 28. Smith, E. R., Tan, S. J., Holt, S. G. & Hewitson, T. D. FGF23 is synthesised locally by renal tubules and
533 activates injury-primed fibroblasts. *Sci. Reports 2017 71* **7**, 1–14 (2017).

534 29. Smith, E. R., Holt, S. G. & Hewitson, T. D. FGF23 activates injury-primed renal fibroblasts via FGFR4-
535 dependent signalling and enhancement of TGF-β autoinduction. *Int. J. Biochem. Cell Biol.* **92**, 63–78
536 (2017).

537 30. Liu, S., Guo, R., Simpson, L. G., Xiao, Z. S., Burnham, C. E. & Quarles, L. D. Regulation of fibroblastic
538 growth factor 23 expression but not degradation by PHEX. *J. Biol. Chem.* **278**, 37419–37426 (2003).

539 31. Yuan, B., Takaiwa, M., Clemens, T. L., Feng, J. Q., Kumar, R., Rowe, P. S., Xie, Y. & Drezner, M. K.
540 Aberrant Phex function in osteoblasts and osteocytes alone underlies murine X-linked
541 hypophosphatemia. *J. Clin. Invest.* **118**, 722–734 (2008).

542 32. Pastor-Arroyo, E. M., Gehring, N., Krudewig, C., Costantino, S., Bettoni, C., Knöpfel, T., Sabrautzki, S.,
543 Lorenz-Depiereux, B., Pastor, J., Strom, T. M., Hrabě de Angelis, M., Camici, G. G., Paneni, F., Wagner,
544 C. A. & Rubio-Aliaga, I. The elevation of circulating fibroblast growth factor 23 without kidney disease
545 does not increase cardiovascular disease risk. *Kidney Int.* **94**, 49–59 (2018).

546 33. Akwo, E., Pike, M. M., Ertuglu, L. A., Vartanian, N., Farber-Eger, E., Lipworth, L., Perwad, F., Siew, E.,
547 Hung, A., Bansal, N., Boer, I. de, Kestenbaum, B., Cox, N. J., Ikizler, T. A., Wells, Q. & Robinson-Cohen,
548 C. Association of Genetically Predicted Fibroblast Growth Factor-23 with Heart Failure A Mendelian
549 Randomization Study. *Clin. J. Am. Soc. Nephrol.* **17**, 1183–1193 (2022).

550 34. Leifheit-Nestler, M., Wagner, M. A., Richter, B., Piepert, C., Eitner, F., Böckmann, I., Vogt, I., Grund, A.,
551 Hille, S. S., Foinquinos, A., Zimmer, K., Thum, T., Müller, O. J. & Haffner, D. Cardiac Fibroblast Growth
552 Factor 23 Excess Does Not Induce Left Ventricular Hypertrophy in Healthy Mice. *Front. Cell Dev. Biol.* **9**,
553 2987 (2021).

554 35. Liu, E. S., Thoonen, R., Petit, E., Yu, B., Buys, E. S., Scherrer-Crosbie, M. & Demay, M. B. Increased
555 Circulating FGF23 Does Not Lead to Cardiac Hypertrophy in the Male Hyp Mouse Model of XLH.
556 *Endocrinology* **159**, 2165–2172 (2018).

557 36. Meaux, M. N., Alioli, C., Linglart, A., Lemoine, S., Vignot, E., Bertholet-Thomas, A., Peyruchaud, O.,
558 Flammier, S., Machuca-Gayet, I. & Bacchetta, J. X-Linked Hypophosphatemia, Not Only a Skeletal
559 Disease But Also a Chronic Inflammatory State. *J. Clin. Endocrinol. Metab.* **107**, 3275–3286 (2022).

560 37. Edmonston, D., Grabner, A. & Wolf, M. FGF23 and klotho at the intersection of kidney and
561 cardiovascular disease. *Nat. Rev. Cardiol. 2023* 1–14 (2023) doi:10.1038/s41569-023-00903-0.

562 38. Kyriakis, J. M. & Avruch, J. Mammalian MAPK signal transduction pathways activated by stress and
563 inflammation: a 10-year update. *Physiol. Rev.* **92**, 689–737 (2012).

564 39. Cargnello, M. & Roux, P. P. Activation and Function of the MAPKs and Their Substrates, the MAPK-
565 Activated Protein Kinases. *Microbiol. Mol. Biol. Rev.* **75**, 50 (2011).

566 40. Grabner, A., Amaral, A. P., Schramm, K., Singh, S., Sloan, A., Yanucil, C., Li, J., Shehadeh, L. A., Hare,
567 J. M., David, V., Martin, A., Fornoni, A., Di Marco, G. S., Kentrup, D., Reuter, S., Mayer, A. B.,
568 Pavenstädt, H., Stypmann, J., Kuhn, C., *et al.* Activation of cardiac fibroblast growth factor receptor 4
569 causes left ventricular hypertrophy. *Cell Metab* **22**, 1020–1032 (2015).

570 41. Cooper, J. A., Sefton, B. M. & Hunter, T. Diverse mitogenic agents induce the phosphorylation of two
571 related 42,000-dalton proteins on tyrosine in quiescent chick cells. *Mol. Cell. Biol.* **4**, 30–37 (1984).

572 42. Chen, R.-H., Sarnecki, C. & Blenis, J. Nuclear localization and regulation of erk- and rsk-encoded protein
573 kinases. *Mol. Cell. Biol.* **12**, 915 (1992).

574 43. Lenormand, P., Sardet, C., Pagès, G., L'Allemain, G., Brunet, A. & Pouysségur, J. Growth factors induce
575 nuclear translocation of MAP kinases (p42mapk and p44mapk) but not of their activator MAP kinase
576 kinase (p45mapkk) in fibroblasts. *J. Cell Biol.* **122**, 1079–1088 (1993).

577 44. Hazzalin, C. A. & Mahadevan, L. C. MAPK-regulated transcription: a continuously variable gene switch?
578 *Nat. Rev. Mol. Cell Biol.* **3**, 30–40 (2002).

579 45. Farrow, E. G., Davis, S. I., Summers, L. J. & White, K. E. Initial FGF23-mediated signaling occurs in the
580 distal convoluted tubule. *J. Am. Soc. Nephrol.* **20**, 955–960 (2009).

581 46. Ranch, D., Zhang, M. Y., Portale, A. A. & Perwad, F. Fibroblast growth factor 23 regulates renal 1,25-
582 dihydroxyvitamin D and phosphate metabolism via the MAP kinase signaling pathway in Hyp mice. *J.*
583 *Bone Miner. Res.* **26**, 1883–90 (2011).

584 47. Lucas, R. M., Luo, L. & Stow, J. L. ERK1/2 in immune signalling. *Biochem. Soc. Trans.* **50**, 1341–1352
585 (2022).

586 48. Ichikawa, S., Austin, A. M., Gray, A. K. & Econs, M. J. A Phex Mutation in a Murine Model of X-linked
587 Hypophosphatemia Alters Phosphate Responsiveness of Bone Cells. *J. Bone Miner. Res.* **27**, 453
588 (2012).

589 49. Sui, T., Yuan, L., Liu, H., Chen, M., Deng, J., Wang, Y., Li, Z. & Lai, L. CRISPR/Cas9-mediated mutation
590 of PHEX in rabbit recapitulates human X-linked hypophosphatemia (XLH). *Hum. Mol. Genet.* **25**, 2661–
591 2671 (2016).

592 50. Böckmann, I., Leifheit-Nestler, M., John, U., Metzing, O., Rehberg, M., Schlingmann, K. P., Weitz, M.,
593 Wühl, E., Sparta, G., Schnabel, D., Hoppe, B. & Haffner, D. #1323 Kidney health in children with X-linked
594 hypophosphatemia: lessons from the prospective multicenter study in Germany and Switzerland.

595 *Nephrol. Dial. Transplant.* **39**, 518–524 (2024).

596 51. Meng, X. M., Nikolic-Paterson, D. J. & Lan, H. Y. TGF-β: the master regulator of fibrosis. *Nat. Rev.*
597 *Nephrol. 2016 126* **12**, 325–338 (2016).

598 52. Moreno, J. A., Izquierdo, M. C., Sanchez-Niño, M. D., Suárez-Alvarez, B., Lopez-Larrea, C., Jakubowski,
599 A., Blanco, J., Ramirez, R., Selgas, R., Ruiz-Ortega, M., Egido, J., Ortiz, A. & Sanz, A. B. The
600 inflammatory cytokines TWEAK and TNFα reduce renal klotho expression through NFκB. *J. Am. Soc.*
601 *Nephrol.* **22**, 1315–1325 (2011).

602 53. Wu, L., Liu, C., Chang, D. Y., Zhan, R., Sun, J., Cui, S. H., Eddy, S., Nair, V., Tanner, E., Brosius, F. C.,
603 Looker, H. C., Nelson, R. G., Kretzler, M., Wang, J. C., Xu, M., Ju, W., Zhao, M. H., Chen, M. & Zheng, L.
604 Annexin A1 alleviates kidney injury by promoting the resolution of inflammation in diabetic nephropathy.
605 *Kidney Int.* **100**, 107–121 (2021).

606 54. Nair, V., Robinson-Cohen, C., Smith, M. R., Bellovich, K. A., Bhat, Z. Y., Bobadilla, M., Brosius, F., De
607 Boer, I. H., Essioux, L., Formentini, I., Gadegbeku, C. A., Gipson, D., Hawkins, J., Himmelfarb, J.,
608 Kestenbaum, B., Kretzler, M., Magnone, M. C., Perumal, K., Steigerwalt, S., *et al.* Growth Differentiation
609 Factor-15 and Risk of CKD Progression. *J. Am. Soc. Nephrol.* **28**, 2233–2240 (2017).

610 55. Hu, M. C., Shi, M., Zhang, J., Pastor, J., Nakatani, T., Lanske, B., Razzaque, M. S., Rosenblatt, K. P.,
611 Baum, M. G., Kuro-O, M. & Moe, O. W. Klotho: a novel phosphaturic substance acting as an autocrine
612 enzyme in the renal proximal tubule. *FASEB J.* **24**, 3438–3450 (2010).

613 56. Li, H., Martin, A., David, V. & Quarles, L. D. Compound deletion of Fgfr3 and Fgfr4 partially rescues the
614 Hyp mouse phenotype. *Am. J. Physiol. Endocrinol. Metab.* **300**, (2011).

615 57. Wöhrle, S., Henninger, C., Bonny, O., Thuery, A., Beluch, N., Hynes, N. E., Guagnano, V., Sellers, W. R.,
616 Hofmann, F., Kneissel, M. & Graus Porta, D. Pharmacological inhibition of fibroblast growth factor (FGF)
617 receptor signaling ameliorates FGF23-mediated hypophosphatemic rickets. *J. Bone Miner. Res.* **28**, 899–
618 911 (2013).

619 58. Xie, Y., Su, N., Yang, J., Tan, Q., Huang, S., Jin, M., Ni, Z., Zhang, B., Zhang, D., Luo, F., Chen, H., Sun,
620 X., Feng, J. Q., Qi, H. & Chen, L. FGF/FGFR signaling in health and disease. *Signal Transduct. Target.*
621 *Ther.* **5**, 181 (2020).

622 59. Xiao, L., Naganawa, T., Lorenzo, J., Carpenter, T. O., Coffin, J. D. & Hurley, M. M. Nuclear isoforms of
623 fibroblast growth factor 2 are novel inducers of hypophosphatemia via modulation of FGF23 and
624 KLOTHO. *J. Biol. Chem.* **285**, 2834–2846 (2010).

625 60. Andrikopoulos, P., Kieswich, J., Pacheco, S., Nadarajah, L., Harwood, S. M., O'Riordan, C. E.,
626 Thiemermann, C. & Yaqoob, M. M. The MEK Inhibitor Trametinib Ameliorates Kidney Fibrosis by
627 Suppressing ERK1/2 and mTORC1 Signaling. *J. Am. Soc. Nephrol.* **30**, 33–49 (2019).

628 61. Das, R., Kim, S.-J., Nguyen, N. T., Kwon, H. J., Cha, S.-K. & Park, K.-S. Inhibition of the ERK1/2-
629 mTORC1 axis ameliorates proteinuria and the fibrogenic action of transforming growth factor-β in
630 Adriamycin-induced glomerulosclerosis. *Kidney Int.* **96**, 927–941 (2019).

631 62. Jo, S.-K., Cho, W. Y., Sung, S. A., Kim, H. K. & Won, N. H. MEK inhibitor, U0126, attenuates cisplatin-
632 induced renal injury by decreasing inflammation and apoptosis. *Kidney Int.* **67**, 458–66 (2005).

63. Agoro, R., Montagna, A., Goetz, R., Aligbe, O., Singh, G., Coe, L. M., Mohammadi, M., Rivella, S. & Sitara, D. Inhibition of fibroblast growth factor 23 (FGF23) signaling rescues renal anemia. *FASEB J.* **32**, 3752–3764 (2018).

64. Courbon, G., Thomas, J. J., Martinez-Calle, M., Wang, X., Spindler, J., Von Drasek, J., Hunt-Tobey, B., Mehta, R., Isakova, T., Chang, W., Creemers, J. W. M., Ji, P., Martin, A. & David, V. Bone-derived C-terminal FGF23 cleaved peptides increase iron availability in acute inflammation. *Blood* **142**, 106–118 (2023).

FIGURE LEGENDS

Fig. 1. Elevated FGF23 levels in Hyp-Duk mice induces sustained-ERK signaling and inflammatory, and immune gene signatures in the kidneys, which are mitigated by cFGF23 gene therapy. A) Graphical illustration showing the experimental design for the *in vivo* experiment. **B)** Mouse iFGF23 levels in the serum of WT and Hyp-Duk mice (n=5, each group). **C)** Human cFGF23 levels in the serum of WT, Hyp-Duk, and Hyp-Duk mice receiving AAV-FGF23 (cFGF23-Hyp-Duk); n=5, each group; ND: not detected. **D)** Volcano plots illustrating DEGs identified by RNA-seq in the kidneys of WT, Hyp-Duk, and cFGF23-Hyp-Duk mice. *Left panel*: DEGs compared between Hyp-Duk versus WT; *right panel*: DEGs compared between cFGF23-Hyp-Duk versus Hyp-Duk. Note that numerous DEGs identified in the kidneys of Hyp-Duk were significantly oppositely regulated in the kidneys of cFGF23-Hyp-Duk mice. **E&F)** Gene expression levels of late- and early-ERK targets in the kidneys of WT, Hyp-Duk, and cFGF23-Hyp-Duk mice. **G)** Percentage of DEGs in the kidneys of Hyp-Duk present in the ImmPort database. **H)** Percentage of ImmPort DEGs in the kidneys of Hyp-Duk rescued by AAV-cFGF23 treatment. **I)** Heatmap of ImmPort DEGs in the kidneys of Hyp-Duk rescued by AAV-cFGF23 treatment (block 1 and 2 represent downregulated and upregulated genes in Hyp-Duk mice, respectively. **J)** Selected significantly upregulated GO pathways (biological processes) in the kidneys of Hyp-Duk versus WT mice. Note that these pathways were either significantly or partially rescued in the kidneys of cFGF23-Hyp-Duk mice. Dotted line indicates threshold for *padj<0.05*. The pathway names in red indicate specific signal transduction pathways implicated in inflammatory and immune gene signatures. **K&L)** Graphs illustrating representative genes implicated in GO pathways of overall inflammatory and immune responses in the kidneys of WT, Hyp-Duk, and cFGF23-Hyp-Duk mice. **M)** Urinary NGAL levels normalized to creatinine. n=5, each group. All values are expressed as arithmetic means ± SE.

Fig. 2. Effects of low versus high FGF23 concentrations (for 15 mins vs. 24 h) on ERK activation and *EGR1* levels. A) Original immunoblots of Klotho, pERK1/2 and tERK1/2 upon treatment with 0.5 nM and 10 nM FGF23 in HEK^{Kl} and HEK^{Wt} cells for 15 min and 24 hrs. **B)** Original immunoblots of pERK1/2 and ERK in HEK^{Kl} cells upon treating with increasing concentrations of FGF23 for 24 hours. **C&D)** Fold change *EGR1* mRNA levels, normalized to *GAPDH* upon treating 0.5 nM and 10 nM FGF23 in HEK^{Kl}/HEK^{Wt} cells over 24 hours, respectively (n=3). *p* values in red and teal indicate comparisons between FGF23 vs control treatment in HEK^{Kl} and HEK^{Wt} cells, respectively. ns=*p*>0.05. **E)** *EGR1* mRNA, normalized to *GAPDH,* upon treating with 0.5 nM and 10 nM FGF23 for 24 hours in HEK^{Kl} cells. n=3, each group. All the values are expressed as arithmetic means ± SE.

Fig. 3. Identification of temporal ERK signaling by physiological versus pathological FGF23 concentrations. A) Graphic illustration showing the experimental design for RNA-seq. **B&C)** Volcano plots illustrating all the genes identified by RNA-seq upon physiological and FGF23 pathological in HEK^{Wt}/HEK^{Kl} cells, respectively. The upregulated and downregulated genes (abs(log2FC)>1) are shown in red and blue, respectively. **D)** ERK targets that are statistically significantly upregulated by physiological FGF23 compared to pathological FGF23 in HEK^{Kl} cells. The gene expression is compared to the corresponding control. **E)** ERK targets that are either statistically significantly unchanged or

upregulated by pathological FGF23 compared to physiological FGF23 in HEK^{KI} cells. The gene expression is compared to the corresponding control. **F)** Venn diagram showing DEGs compared between physiological FGF23 and pathological FGF23 in HEK^{KI} cells (padj<0.05; (abs(log2FC)>1). **G)** Selected upregulated GO pathways in biological processes enriched upon pathological FGF23 in HEK^{KI} cells (padj<0.05; log2Fc>1). The red arrows indicate pathways implicated in inflammatory and immune gene signatures. **H)** Heatmap highlighting DEGs by pathological FGF23 in HEK^{KI} cells that were present in the ImmPort database. Block 1 represents DEGs only affected by pathological FGF23, while block 2 represents DEGs affected by both pathological and physiological FGF23. Exemplary immune/inflammatory genes reported in literature are shown in red. **I)** Representative transcripts implicated in inflammatory and immune gene signature and upregulated only by pathological FGF23 in HEK^{KI} cells (red bars). Note that these genes are unchanged by similar treatment in HEK^{Wt} cells (grey bars). (n=3), ns=padj>0.05. All the values are expressed as arithmetic means ± SE.

Fig. 4. Pathological FGF23-mediated ERK signaling, inflammatory and immune gene signatures are inhibited by FGFR and MEK blockers. A) *EGR1* and *ETV4* mRNA, normalized to *GAPDH*, upon treating HEK^{KI} cells with 10 nM FGF23 for 24 hours with or without FGFR inhibitor (PD173074) or MEK inhibitor (U0126) (n=3). **B)** mRNA levels of *TNFRSF9*, *TNFRSF12A*, *GDF15*, *ANXA1*, and *TGFB1* normalized to *GAPDH*, upon treating HEK^{KI} cells with pathological FGF23 (10 nM FGF23 for 24 hours) with or without FGFR inhibitor or MEK inhibitor (n=3). All values are expressed as arithmetic means ± SE.

Fig. 5. Pathological FGF23-mediated ERK signaling, inflammatory and immune gene signature is mitigated by cFGF23. A) Graphical illustration showing mechanisms of action of the cFGF23 peptide. *Left panel:* Intact full-length iFGF23 harbors its C-terminus cFGF23 and N-terminus nFGF23. Within iFGF23, cFGF23 and nFGF23 bind with co-receptors Klotho and FGFR, respectively, and activate ERK signaling. *Right panel:* High concentration of the cFGF23 peptide competes with iFGF23 for binding with Klotho and thus mitigates ERK signaling. **B)** *EGR1* and *ETV4* mRNA, normalized to *GAPDH*, upon treating HEK^{KI} cells with pathological FGF23 (10 nM FGF23 for 24 hours) with or without increasing concentrations of cFGF23 (n=3). **C)** mRNA levels of *TNFRSF9*, *TNFRSF12A*, *GDF15*, *ANXA1*, and *TGFB1* normalized to *GAPDH*, upon treating HEK^{KI} cells with pathological FGF23 with or without increasing concentrations of cFGF23 (n=3). All values are expressed as arithmetic means ± SE.

Fig. 6. Proposed model: Left Panel: In diseases where FGF23 is chronically elevated, the FGF23-FGFR-Klotho-HS signaling complex induces sustained-ERK activation in the cytoplasm. ERK is continuously and irreversibly translocated to the nucleus, where it upregulates late-ERK targets along with inflammation and immune gene signatures. It is currently unclear whether late-ERK targets directly activate inflammation and immune gene signatures. The cFGF23 peptide blocks FGF23-Klotho binding, thereby inhibiting downstream ERK signaling as well as inflammation and immune gene signatures.
Right Panel: Physiological rise in FGF23 rapidly and reversibly activate ERK in the cytoplasm via FGF23-FGFR-Klotho-HS signaling complex. In this case, ERK transiently translocates to the nucleus and upregulates early-ERK targets and is less likely to regulate gene signatures implicated in inflammation and immune responses.

Fig. 1

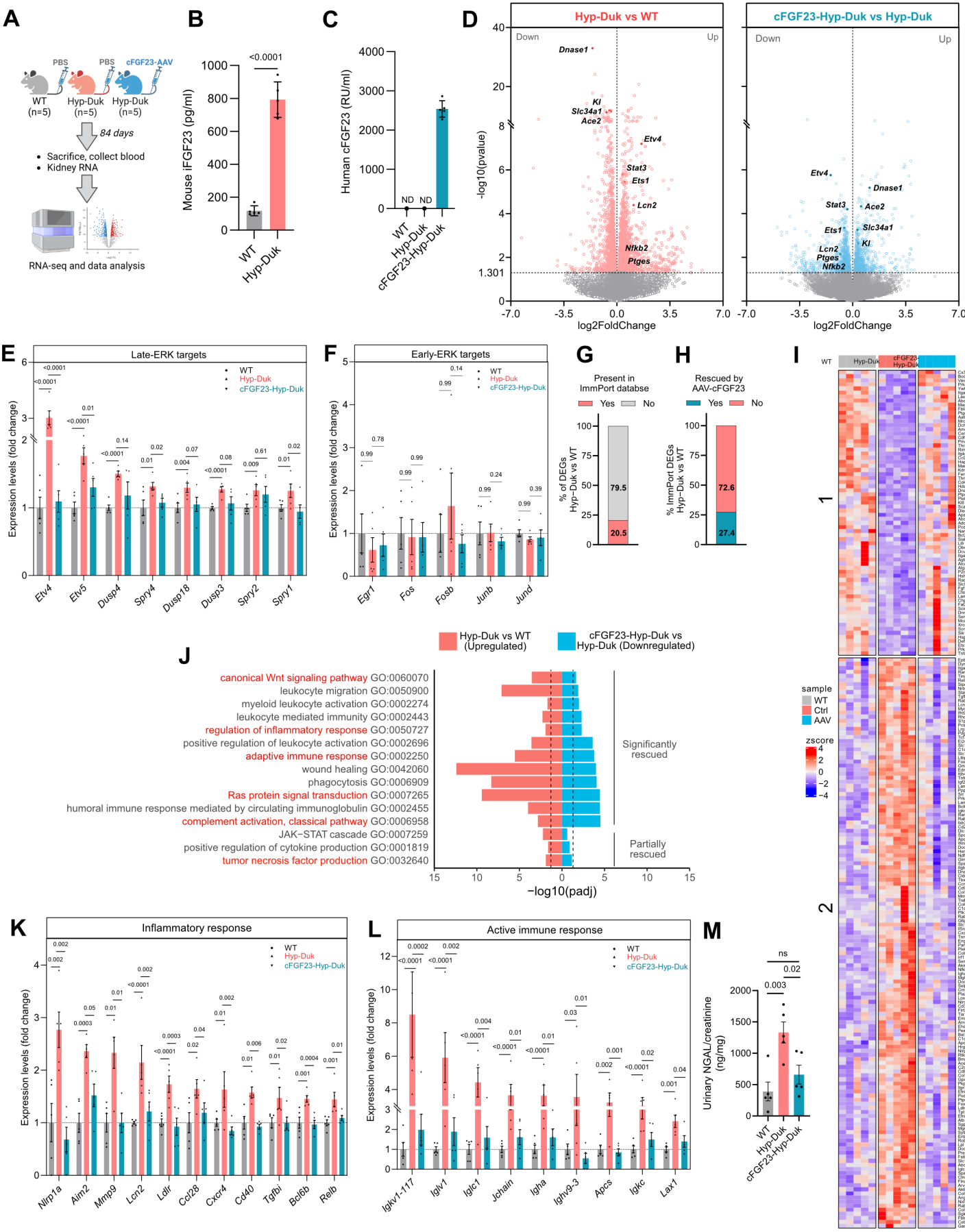
A
PBS
PBS
cFGF23-AAV
WT (n=5)
Hyp-Duk (n=5)
Hyp-Duk (n=5)
84 days
Sacrifice, collect blood
Kidney RNA
RNA-seq and data analysis
B
Mouse iFGF23 (pg/ml)
<0.0001
WT
Hyp-Duk
C
Human cFGF23 (RU/ml)
ND
ND
WT
Hyp-Duk
cFGF23-Hyp-Duk
D
Hyp-Duk vs WT
cFGF23-Hyp-Duk vs Hyp-Duk
Down
Up
-log10(pvalue)
log2FoldChange
Dnase1
Kl
Slc34a1
Ace2
Etv4
Stat3
Ets1
Lcn2
Nfkb2
Ptges
1.301
E
Late-ERK targets
Expression levels (fold change)
WT
Hyp-Duk
cFGF23-Hyp-Duk
Etv4
Etv5
Dusp4
Spry4
Dusp18
Dusp3
Spry2
Spry1
F
Early-ERK targets
Egr1
Fos
Fosb
Junb
Jund
G
Present in ImmPort databse
Yes
No
% of DEGs Hyp−Duk vs WT
79.5
20.5
H
Rescued by AAV-cFGF23
% ImmPort DEGs Hyp−Duk vs WT
72.6
27.4
I
WT
Hyp-Duk
cFGF23-Hyp-Duk
sample
WT
Ctrl
AAV
zscore
J
Hyp-Duk vs WT (Upregulated)
cFGF23-Hyp-Duk vs Hyp-Duk (Downregulated)
canonical Wnt signaling pathway GO:0060070
leukocyte migration GO:0050900
myeloid leukocyte activation GO:0002274
leukocyte mediated immunity GO:0002443
regulation of inflammatory response GO:0050727
positive regulation of leukocyte activation GO:0002696
adaptive immune response GO:0002250
wound healing GO:0042060
phagocytosis GO:0006909
Ras protein signal transduction GO:0007265
humoral immune response mediated by circulating immunoglobulin GO:0002455
complement activation, classical pathway GO:0006958
JAK−STAT cascade GO:0007259
positive regulation of cytokine production GO:0001819
tumor necrosis factor production GO:0032640
Significantly rescued
Partially rescued
−log10(padj)
K
Inflammatory response
Expression levels (fold change)
WT
Hyp-Duk
cFGF23-Hyp-Duk
Nlrp1a
Aim2
Mmp9
Lcn2
Ldlr
Col28
Cxcr4
Cd40
Tgfbi
Bcl6b
Relb
L
Active immune response
Expression levels (fold change)
WT
Hyp-Duk
cFGF23-Hyp-Duk
Igkv1-117
Iglv1
Iglc1
Jchain
Igha
Ighv9-3
Apcs
Igkc
Lax1
M
Urinary NGAL/creatinine (ng/mg)
ns
0.02
0.003
WT
Hyp-Duk
cFGF23-Hyp-Duk

Fig. 2

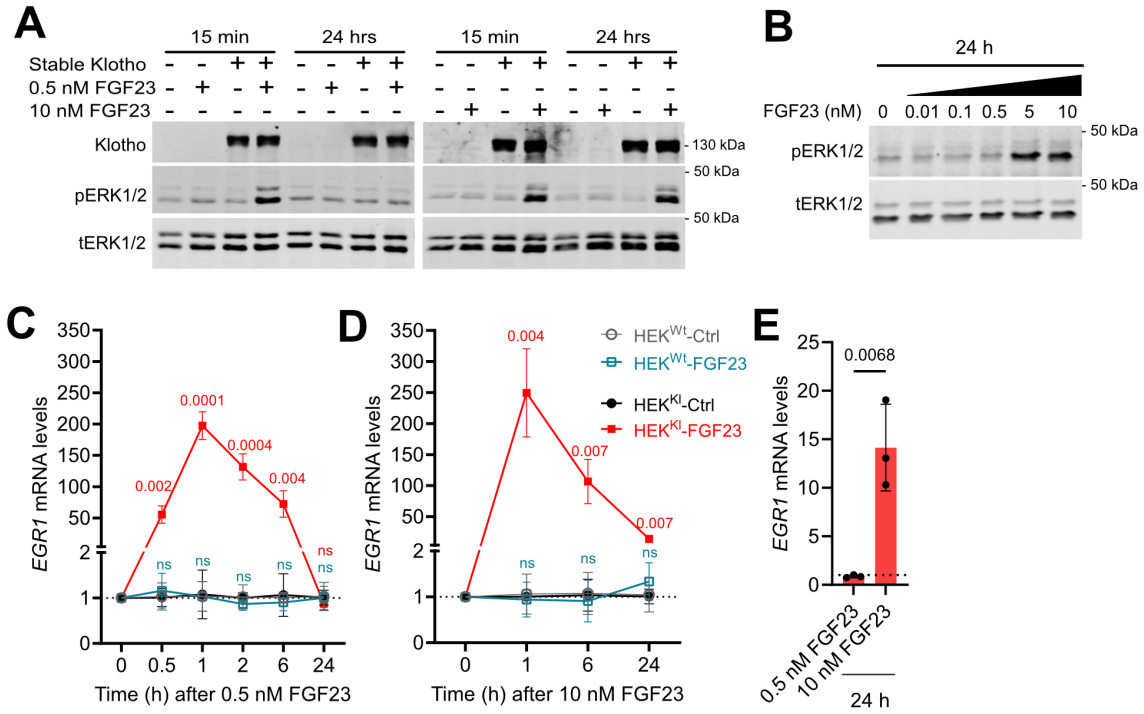
A
15 min
24 hrs
15 min
24 hrs
Stable Klotho
0.5 nM FGF23
10 nM FGF23
Klotho
pERK1/2
tERK1/2
130 kDa
50 kDa
50 kDa
B
24 h
FGF23 (nM) 0 0.01 0.1 0.5 5 10
pERK1/2
tERK1/2
50 kDa
50 kDa
C
EGR1 mRNA levels
0.002
0.0001
0.0004
0.004
ns
Time (h) after 0.5 nM FGF23
D
HEKWt-Ctrl
HEKWt-FGF23
HEKKI-Ctrl
HEKKI-FGF23
0.004
0.007
0.007
Time (h) after 10 nM FGF23
E
0.0068
0.5 nM FGF23
10 nM FGF23
24 h

Fig. 3

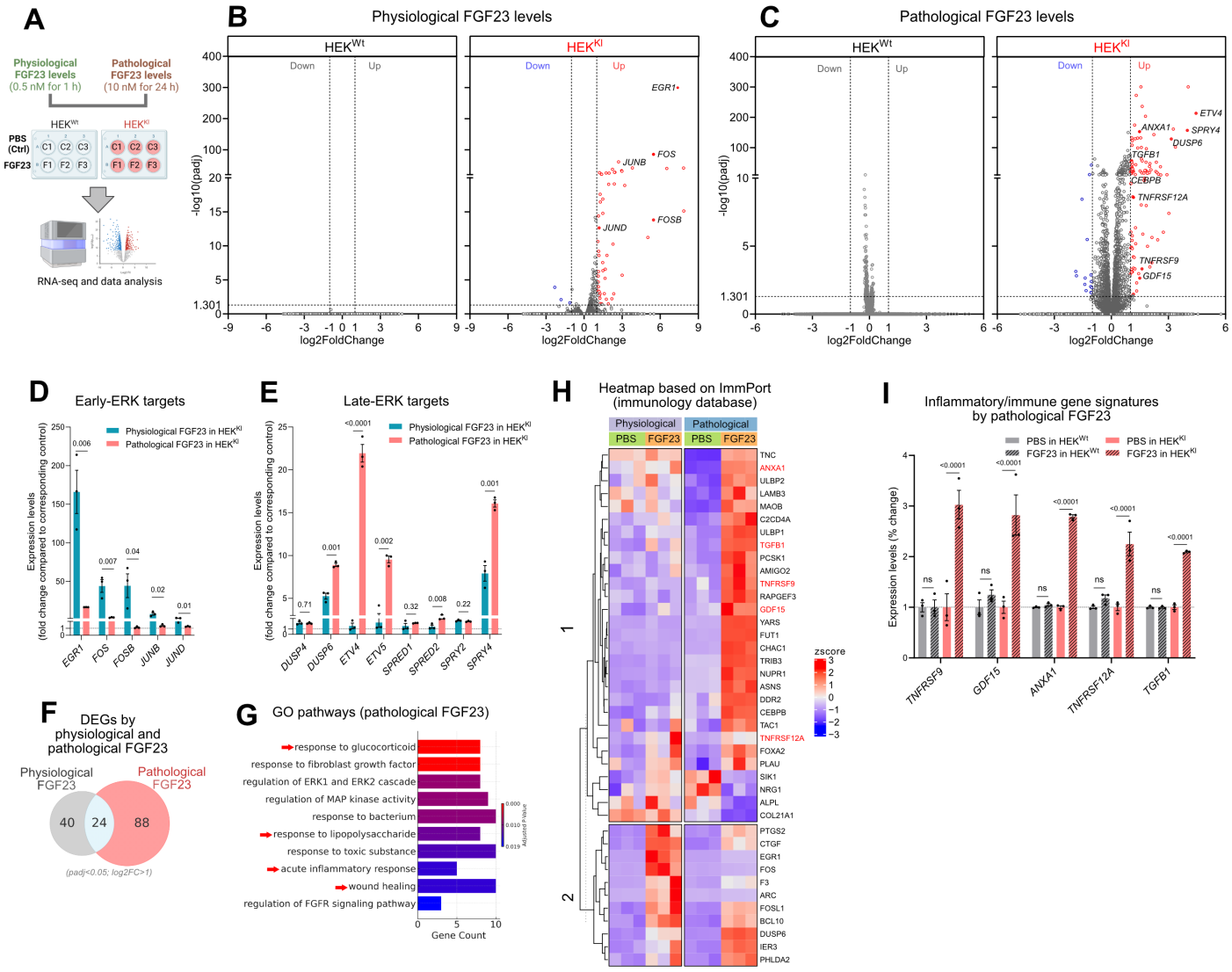
A
Physiological FGF23 levels (0.5 nM for 1 h)
Pathological FGF23 levels (10 nM for 24 h)
HEKWt
HEKKI
PBS (Ctrl)
FGF23
RNA-seq and data analysis
B
Physiological FGF23 levels
HEKWt
HEKKI
Down
Up
EGR1
FOS
JUNB
JUND
FOSB
-log10(padj)
log2FoldChange
C
Pathological FGF23 levels
ETV4
ANXA1
SPRY4
DUSP6
TGFB1
CEBPB
TNFRSF12A
TNFRSF9
GDF15
D
Early-ERK targets
Physiological FGF23 in HEKKI
Pathological FGF23 in HEKKI
Expression levels (fold change compared to corresponding control)
EGR1
FOS
FOSB
JUNB
JUND
E
Late-ERK targets
DUSP4
DUSP6
ETV4
ETV5
SPRED1
SPRED2
SPRY2
SPRY4
F
DEGs by physiological and pathological FGF23
Physiological FGF23
Pathological FGF23
40
24
88
(padj<0.05; log2FC>1)
G
GO pathways (pathological FGF23)
response to glucocorticoid
response to fibroblast growth factor
regulation of ERK1 and ERK2 cascade
regulation of MAP kinase activity
response to bacterium
response to lipopolysaccharide
response to toxic substance
acute inflammatory response
wound healing
regulation of FGFR signaling pathway
Gene Count
Adjusted P-value
H
Heatmap based on ImmPort (immunology database)
Physiological
Pathological
PBS
FGF23
zscore
TNC
ANXA1
ULBP2
LAMB3
MAOB
C2CD4A
ULBP1
TGFB1
PCSK1
AMIGO2
TNFRSF9
RAPGEF3
GDF15
YARS
FUT1
CHAC1
TRIB3
NUPR1
ASNS
DDR2
CEBPB
TAC1
TNFRSF12A
FOXA2
PLAU
SIK1
NRG1
ALPL
COL21A1
PTGS2
CTGF
EGR1
FOS
F3
ARC
FOSL1
BCL10
DUSP6
IER3
PHLDA2
I
Inflammatory/immune gene signatures by pathological FGF23
PBS in HEKWt
FGF23 in HEKWt
PBS in HEKKI
FGF23 in HEKKI
Expression levels (% change)
TNFRSF9
GDF15
ANXA1
TNFRSF12A
TGFB1

Fig. 4

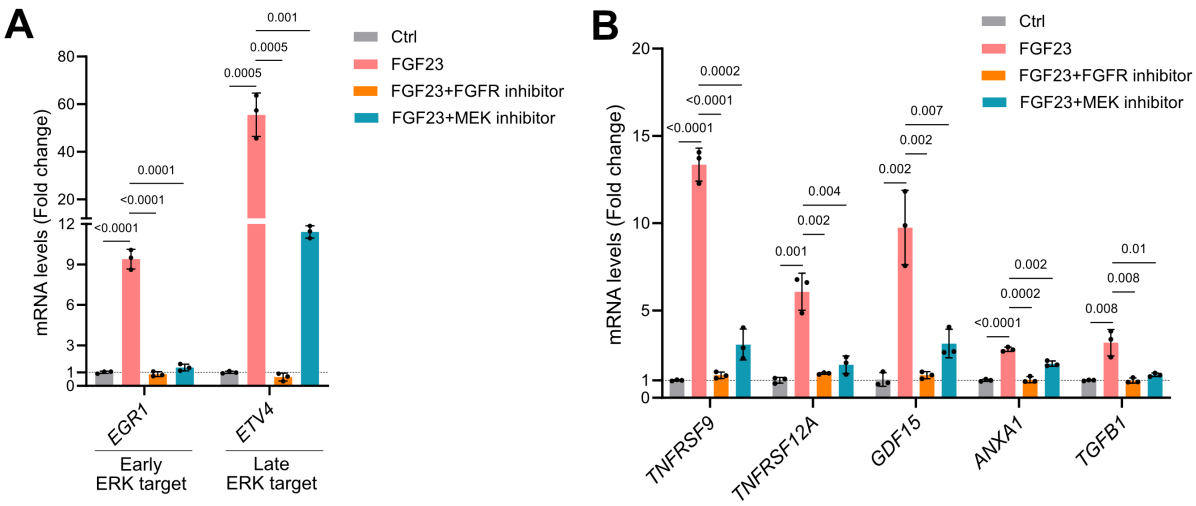
A
mRNA levels (Fold change)
80
60
40
20
12
9
6
3
1
0
<0.0001
<0.0001
0.0001
0.0005
0.0005
0.001
EGR1
ETV4
Early ERK target
Late ERK target
Ctrl
FGF23
FGF23+FGFR inhibitor
FGF23+MEK inhibitor
B
mRNA levels (Fold change)
20
15
10
5
1
0
<0.0001
<0.0001
0.0002
0.001
0.002
0.004
0.002
0.002
0.002
0.007
<0.0001
0.0002
0.002
0.008
0.008
0.01
TNFRSF9
TNFRSF12A
GDF15
ANXA1
TGFB1
Ctrl
FGF23
FGF23+FGFR inhibitor
FGF23+MEK inhibitor

Fig. 5

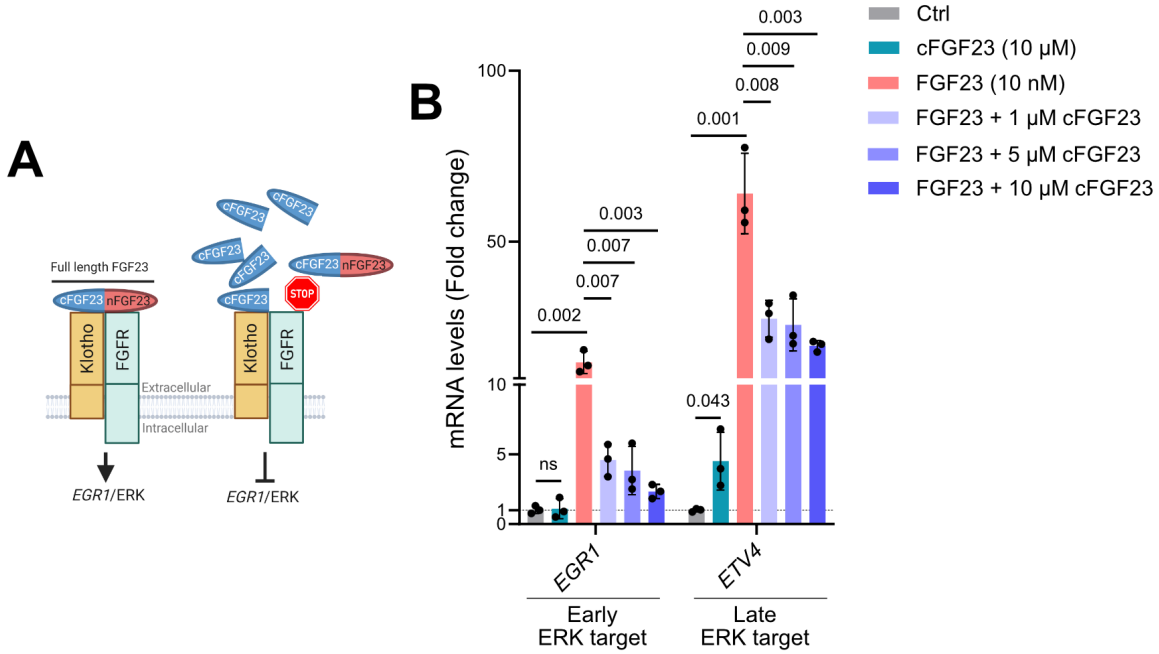
A
Full length FGF23
cFGF23
nFGF23
Klotho
FGFR
Extracellular
Intracellular
EGR1/ERK
STOP
B
mRNA levels (Fold change)
100
50
10
5
1
0
ns
0.002
0.007
0.007
0.003
0.043
0.001
0.008
0.009
0.003
EGR1
ETV4
Early ERK target
Late ERK target
Ctrl
cFGF23 (10 µM)
FGF23 (10 nM)
FGF23 + 1 µM cFGF23
FGF23 + 5 µM cFGF23
FGF23 + 10 µM cFGF23

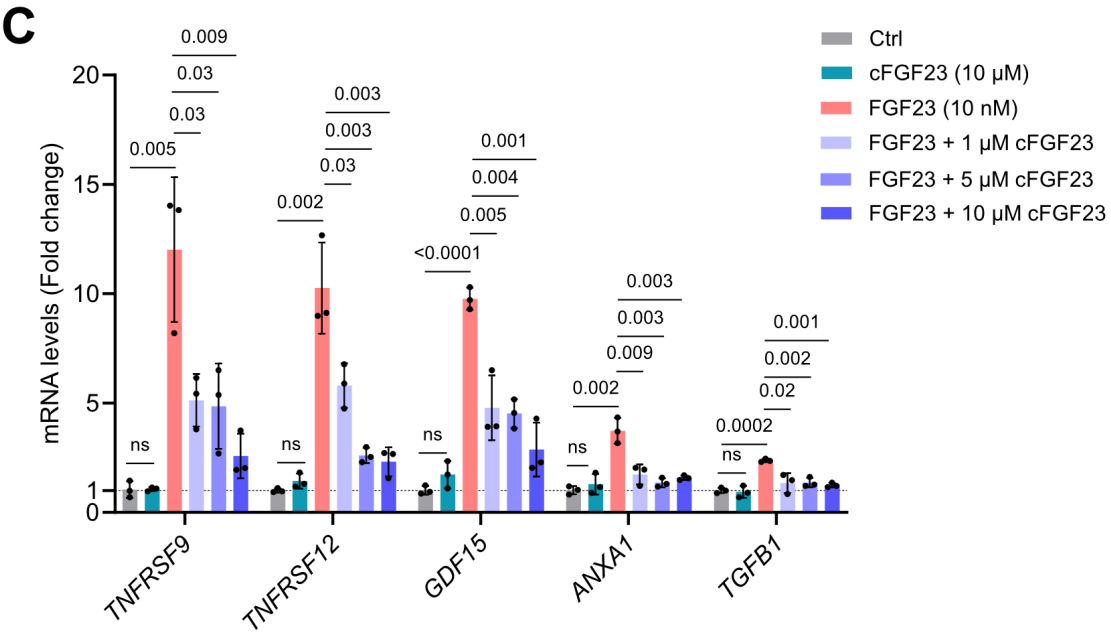
C
mRNA levels (Fold change)
20
15
10
5
1
0
ns
0.005
0.03
0.03
0.009
ns
0.002
0.03
0.003
0.003
ns
<0.0001
0.005
0.004
0.001
ns
0.002
0.009
0.003
0.003
0.0002
ns
0.02
0.002
0.001
TNFRSF9
TNFRSF12
GDF15
ANXA1
TGFB1
Ctrl
cFGF23 (10 µM)
FGF23 (10 nM)
FGF23 + 1 µM cFGF23
FGF23 + 5 µM cFGF23
FGF23 + 10 µM cFGF23

Fig. 6

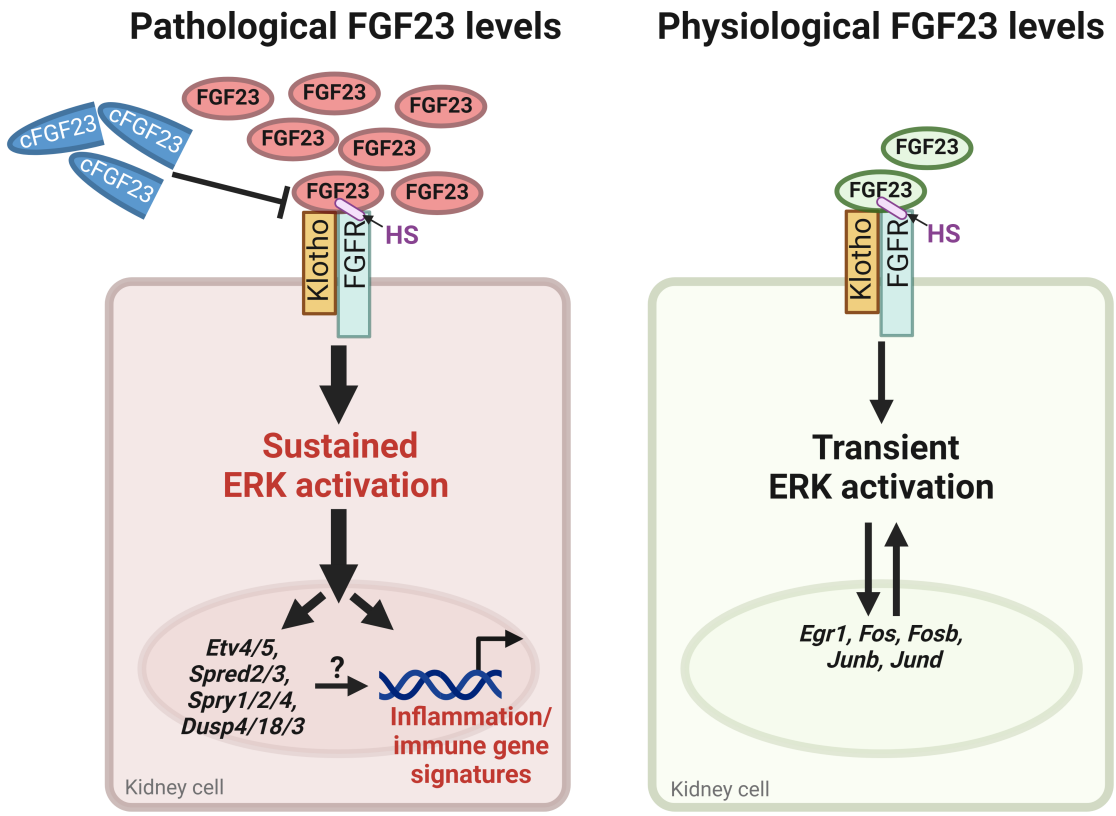
Pathological FGF23 levels
Physiological FGF23 levels
FGF23
cFGF23
HS
Klotho
FGFR
Sustained
ERK activation
Etv4/5,
Spred2/3,
Spry1/2/4,
Dusp4/18/3
?
Inflammation/
immune gene
signatures
Kidney cell
Transient
ERK activation
Egr1, Fos, Fosb,
Junb, Jund
Kidney cell